Electronic Supplementary Information

4D-π-1A Type β-Substituted Zn^{II}-Porphyrins: Ideal Green Sensitizers for Building-Integrated Photovoltaics

A. Covezzi,[a] A. Orbelli Biroli,[b] F. Tessore,[a] A. Forni,[b] D. Marinotto,[a] P.Biagini,[c] G. Di Carlo,[a,*] M. Pizzotti.[a]

[a]Department of Chemistry, University of Milan, INSTM Research Unit, Via C. Golgi 19, 20133 Milano (Italy). E-mail: gabriele.dicarlo@unimi.it

[b]Istituto di Scienze e Tecnologie Molecolari del CNR (CNR-ISTM), SmartMatLab Centre, Via Golgi 19, 20133 Milano, Italy.

[c]Research Center for Renewable Energy & Environmental, Istituto Donegani, ENI S.p.A., via Fauser 4, I-28100, Novara, Italy.

Table of Contents

1) Materials and Methods

All reagents and solvents used in the synthesis were purchased by Sigma Aldrich and used as received, except Et_3N, (freshly distilled over KOH), THF (freshly distilled from Na/benzophenone under nitrogen atmosphere). Silica gel for gravimetric chromatography (Geduran Si 60, 63-200 μm) and for flash chromatography (Geduran Si 60, 40-63 μm) was purchased by Merck. Glassware has been flame-dried under vacuum before use when necessary. Microwave assisted reactions were performed using a Milestone MicroSYNTH instrument. ^{1}H-NMR spectra were recorded on a Bruker Avance DRX-400 and on a Bruker AMX 300 in $CDCl_3$ as solvent with addition, when necessary, of a drop of pyridine-d_5 or in THF-d_8 (Cambridge Isotope Laboratories, Inc.). Mass spectra were obtained with a VG Autospec M246 magnetic mass spectrometer with a LSIMS ionic source. IR spectra were recorded on a Perkin Elmer Spectrum BX spectrophotometer. A drop of a dichloromethane solution of the dye was laid on a sodium chloride plate and allowed to dry, before covering with another sodium chloride plate. The spectral range was 500-4000 cm-1, and the spectra were acquired after 8 scans. Elemental analysis was carried out with a Perkin-Elmer CHN 2400 instrument in the Analytical Laboratories of the Department of Chemistry at the University of Milan.

2) Synthesis of Zn-1; G1 and G2

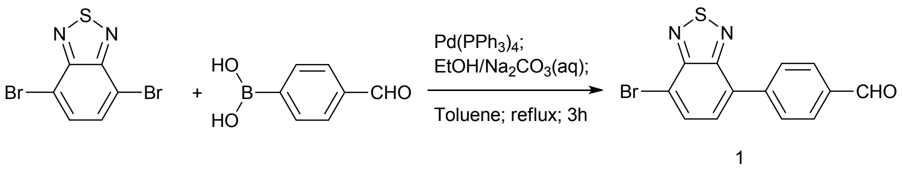

Scheme S1: Synthesis of 4-(7-bromobenzo[1,2,5]thiadiazol-4-yl)benzaldehyde (1)

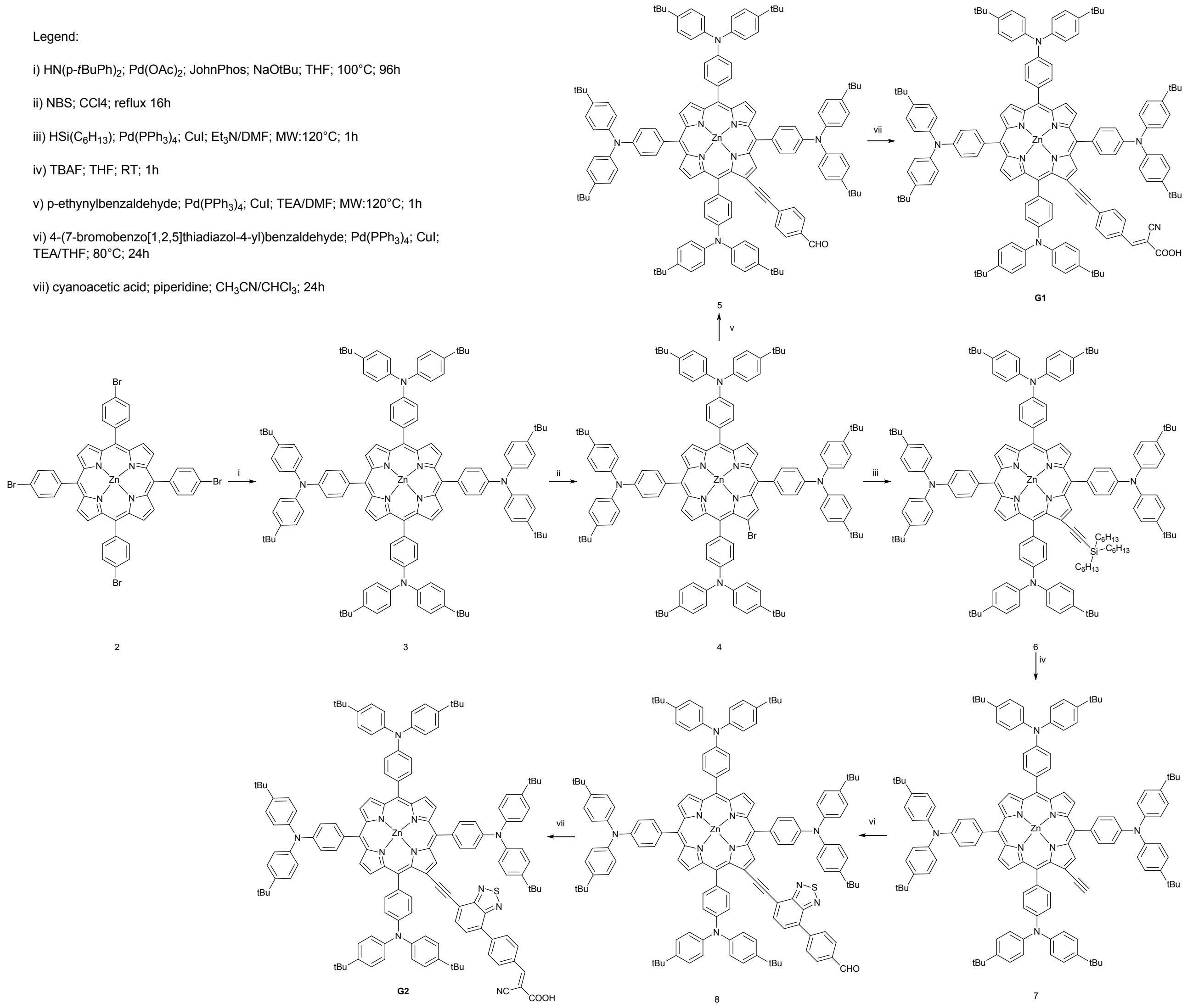

Scheme S2: Synthetic Pathway of G1 and G2 Porphyrinic Dyes

Synthesis of 4-(7-bromobenzo[1,2,5]thiadiazol-4-yl)benzaldehyde (1)

800 mg of 4,7-dibromobenzo[1,2,5]thiadiazole (2.72 mmol), 405 mg of 4-(formylphenyl)boronic acid (2.72 mmol), 62.9 mg of $Pd(PPh_3)_4$ (0.0544 mmol) and 40 mL of anhydrous toluene were added to a dry Schlenk tube and degassed with freeze-pump thaw cycles at -78°C. 12 mL of ethanol and 20 mL of a 2M aqueous solution of Na_2CO_3 were prepared in two different Schlenk tubes, degassed with freeze-pump thaw cycles at -78°C and added separately to the first solution. The obtained solution was refluxed at 116°C for 3 h, then washed with CH_2Cl_2 and H_2O and the organic phase was dried over Na_2SO_4. The solvent was removed under *vacuum* and the crude purified by flash-chromatography (CH_2Cl_2/*n*-Hexane 1/1), leading to 352 mg of a yellow powder (41% yield). ^{1}H-NMR (400 MHz, $CDCl_3$, 25°C): δ = 10.13 (s, 1H), 8.11 (d, 2H), 8.06 (d, 2H), 7.99 (d, 1H), 7.68 ppm (d, 1H).

Synthesis of 2

2.00 g of 4-bromobenzaldehyde (10.8 mmol) and 725 mg of freshly distilled pyrrole (10.8 mmol) were dissolved in 600 mL of CH_2Cl_2 in a round-bottom flask. Nitrogen was bubbled through the mixture in the dark for 15 minutes and 0.77 mL of trifluoroacetic acid (9.72 mmol) were added dropwise. Nitrogen was bubbled for further 10 minutes and the mixture was allowed to react in the dark for 3 hours. 3.68 g of DDQ (16.2 mmol) were added and the mixture stirred in the light for 1 hour. 5.4 mL of NEt_3 (38.9 mmol) were added to quench the reaction and the solution was stirred overnight. The solvent was removed under *vacuum* and the crude purified by column chromatography ($CHCl_3$/*n*-Hexane 4/6). The free-based porphyrin was obtained as a purple powder (845 mg, 34% yield).^{1}H-NMR (400 MHz, $CDCl_3$, 25°C): δ = 8.86 (s, 8H), 8.08 (d, 8H), 7.92 (d, 8H), -2.83 ppm (s, 2H).

373 mg of free-based porphyrin (0.401 mmol) were dissolved in 200 mL of $CHCl_3$ in a two-neck round-bottom flask and heated to reflux. A solution of 194 mg of $Zn(OAc)_2 \cdot 2H_2O$ (0.882 mmol) in methanol was added dropwise and the obtained mixture refluxed for 2 hours at 77°C. The solvent was removed under *vacuum* and the Zn^{II} porphyrin obtained as a purple powder by washing and filtering the solid with H_2O milliQ (365 mg, 92% yield).^{1}H-NMR (400 MHz, $CDCl_3$, 25°C): δ = 8.94 (s, 8H), 8.09 (d, 8H), 7.91 ppm (d, 8H).

Synthesis of 3

616 mg of **2** (0.620 mmol), 953 mg of NaO*t*Bu (9.92 mmol), 27,8 mg of $Pd(OAc)_2$ (0.124 mmol), 74.0 mg of JohnPhos (0.248 mmol) and 31 mL of dry THF were loaded to a dry Schlenk tube. The

mixture was degassed with freeze-pump thaw cycles at -78°C, then 2.79 g of bis(4-(*tert*-butyl)phenyl)amine (9.92 mmol) and 31 mL of dry THF were added. The mixture was degassed again with freeze-pump thaw cycles at -78°C and heated to reflux at 100°C for 96 hours. The solvent was removed under *vacuum* and the crude washed with AcOEt and H_2O. The organic phase was dried over Na_2SO_4, then filtered. The solvent was removed under *vacuum* and the pure product was obtained by column chromatography (CH_2Cl_2/*n*-Hexane 4/6) as a dark powder (453 mg, 41% yield).^{1}H-NMR (400 MHz, $CDCl_3$, 25°C): δ = 9.14 (s, 8H), 8.10 (d, 8H), 7.49 (d, 16H), 7.46 (d, 8H), 7.38 (d, 16H), 1.43 (s, 72H).

Synthesis of 4

126 mg of **3** (0.0699 mmol) were dissolved in a round-bottom flask with 70 mL of CCl_4 and the mixture heated at 80°C. 14.8 mg of NBS (0.0840 mmol) were added and the solution refluxed overnight. The solvent was removed under *vacuum* and the crude washed and filtrated with MeOH leading to a dark powder which was further purified by column chromatography (Toluene/*n*-Hexane 3/7). (75 mg, 56% yield).^{1}H-NMR (400 MHz, $CDCl_3$, 25 °C): δ = 9.14 (s, 1H), 9.03-8.97 (m, 6H), 8.11-8.03 (m, 6H), 7.90-7.79 (m, 2H), 7.51-7.44 (m, 24H), 7.40-7.34 (m, 16H), 1.42 ppm (s, 72H).

Synthesis of 5

In a microwave quartz vessel 87.8 mg of **4** (0.047 mmol), 6.20 mg of $Pd(PPh_3)_4$ (0.0047 mmol), 12 mL of freshly distilled TEA over KOH and 4 mL of DMF were loaded under nitrogen flow. 24.1 mg of *p*-ethynylbenzaldehyde (0.019 mmol) and 1.30 mg of CuI (0.007 mmol) were added to the mixture. The reactor was allowed to react in the microwave cavity for 1 h at 120°C, then the solvents were removed under *vacuum* and the crude purified by column chromatography (CH_2Cl_2/*n*-Hexane 3/7). The pure product was obtained as a dark powder (58 mg, 65% yield). ^{1}H-NMR (300 MHz, THF, 25 °C): δ = 10.07 (s, 1H), 9.35 (s, 1H), 8.95 (m, 6H), 7.97 (m, 12H), 7.47 (m, 20H), 7.36 (m, 16H), 7.03 (d, 4H), 1.42 ppm (s, 72H).

Synthesis of G1

35.5 mg of **5** (0.0185 mmol) were dissolved in 1.15 mL of $CHCl_3$ in a Schlenk tube. 8.50 mg of cyanoacetic acid (0.100 mmol) dissolved in 0.45 mL of CH_3CN and 0.01 mL of piperidine were added and the mixture heated at 80°C overnight. The mixture was washed with an aqueous H_3PO_4 2M solution and CH_2Cl_2 and the organic phase was dried over Na_2SO_4. The solvent was removed under *vacuum* and the crude purified by column chromatography (CH_2Cl_2/MeOH 9/1). The pure product was recovered by washing and filtering with H_2O MilliQ, leading to 30.3 mg of dark green powder (82% yield). ^{1}H-NMR (300 MHz, THF, 25 °C): δ = 9.35 (s, 1H), 8.95 (m, 6H), 8.28 (d, 2H), 8.06 (d, 6H), 7.96 (d, 2H), 7.82 (d, 2H), 7.41 (m, 40H), 7.10 (d, 4H), 1.40 ppm (d, 72H). IR (Neat, cm^{-1}): 2189 (C≡N), 1593 (C=O), 1504, 1359, 1320, 1267, 1182, 1108, 999830, 737. IR (Neat, cm^{-1}): 2196 (C≡N), 1598 (C=O), 1504, 1364, 1321, 1267, 1184, 1110, 998, 831, 737. MS-FAB(+) *m/z*: calcd (%) for $C_{136}H_{133}N_9O_2Zn$ 1991, found 1992 $[M+H]^+$. elemental analysis calcd (%) for $C_{136}H_{133}N_9O_2Zn$: C 82.04, H 6.73, N 6.33; found C 82.19, H 6.72 N 6.64.

Synthesis of 6

In a microwave quartz vessel 200 mg of **4** (0.108 mmol), 25.7 mg of $Pd(PPh_3)_4$ (0.0216 mmol), 15 mL of TEA and 5 mL of DMF were loaded under nitrogen. 167 mg of ethynyltrihexylsilane (0.540 mmol) and 6 mg of CuI (0.0324 mmol) were added and the mixture was allowed to react in the microwave cavity for 1 h at 120°C, then the solvents were removed under *vacuum* and the crude purified by flash chromatography (Toluene/*n*-Hexane 3/7). The pure product was obtained as a dark powder (172.4 mg, 76% yield).^{1}H-NMR (400 MHz, $CDCl_3$, 25 °C): δ = 9.38 (s, 1H), 9.12 (d, 4H), 9.07 (d, 1H), 8.90 (d, 1H), 8.10 (d, 6H), 7.95 (d, 2H), 7.49-7.37 (m, 32H), 1.44 (s, 72H), 1.43-0.86 ppm (m, 39H).

Synthesis of 7

86.2 mg of **6** (0.0410 mmol) were dissolved in 5.2 mL of THF in a Schlenk tube under nitrogen flow, then 0.05 mL of TBAF were added dropwise and the mixture was allowed to react for 1 hour at room temperature. The mixture was washed with CH_2Cl_2 and H_2O and the organic phase dried over Na_2SO_4. The solvent was removed under *vacuum* and the pure product recovered quantitatively (74.6 mg).^{1}H-NMR (400 MHz, $CDCl_3$, 25 °C): δ = 9.42 (s, 1H), 9.08 (m, 6H), 8.08-8.05 (m, 6H), 7.97 (d, 2H), 7.48-7.42 (m, 24H), 7.40-7.36 (m, 16H), 3.64 (s, 1H), 1.46-1.27 ppm (m, 72H).

Synthesis of 8

74.6 mg of **7** (0,0410 mmol), 26.2 mg of (**1**) (0.0820 mmol) and 7.10 mg of $Pd(PPh_3)_4$ (0.00615 mmol) were dissolved in a Schlenk tube with 2.5 mL of THF and 2.5 mL of TEA under nitrogen flow. 0.780 mg of CuI (0.00410 mmol) were added and the mixture heated for 24 hours at 80°C. The solvent was removed under *vacuum* and the crude purified by column chromatography

(CH_2Cl_2/Petroleum Ether 1/1). The pure product was obtained as a dark green powder (61.7 mg, 73% yield).^{1}H-NMR (400 MHz, THF, 25 °C): δ = 10.12 (s, 1H), 9.45 (s, 1H), 9.04 (d, 4H), 8.98 (d, 1H), 8.91 (d, 1H), 8.25 (d, 2H), 8.11 (d, 2H), 8.08 (d, 2H), 8.08-8.03 (m, 8H), 7.58-7.37 (m, 30 H), 7.35 (d, 2H), 7.13 (d, 4H), 6.82 (d, 4H), 1.42-1.23 ppm (m, 72H).

Synthesis of G2

61.7 mg of **8** (0.0299 mmol) were dissolved in 1.5 mL of $CHCl_3$ in a Schlenk tube. 13.0 mg of cyanoacetic acid (0.150 mmol) dissolved in 0.75 mL of CH_3CN and 0.02 mL piperidine were added and the mixture heated at 80°C overnight. The mixture was washed with an aqueous H_3PO_4 2M solution and CH_2Cl_2 and the organic phase was dried over Na_2SO_4. The solvent was removed under *vacuum* and the crude purified by column chromatography (CH_2Cl_2/MeOH 95/5). The pure product was recovered by washing and filtering with H_2O MilliQ, leading to 63.5 g of a dark green powder (98% yield). ^{1}H-NMR (400 MHz, THF, 22 °C): δ = 9.42 (s, 1H), 9.01 (s, 4H), 8.95 (d, 1H), 8.88 (d, 1H), 8.50 (s, 1H), 8.29 (s, 4H), 8.12-7.99 (m, 10H), 7.56-7.33 (m, 30 H), 7.22 (d, 2H), 7.14 (d, 4H), 6.83 (d, 4H), 1.42-1.22 ppm (m, 72H). IR (Neat, cm^{-1}): 2189 (C≡N), 1593 (C=O), 1504, 1359, 1320, 1267, 1182, 1108, 999, 830, 737. MS-FAB(+) *m/z*: calcd for $C_{142}H_{135}N_{11}O_2SZn$ 2125 [M], found 2126 $[M+H]^+$. elemental analysis calcd (%) for $C_{142}H_{135}N_{11}O_2SZn$: C 80.26, H 6.40, N 7.25; found C 80.38, H 6.38, N 7.26.

3) Electronic Absorption and Fluorescence Emission Spectroscopy

Electronic absorption spectra were recorded at room temperature in THF solution, using a Shimadzu UV3600 spectrophotometer and quarz *couvettes* with 1 cm optical path length.

Photoluminescence experiments were carried out at room temperature, after N_2 bubbling for 60 s.

Photoluminescence quantum yields were measured with a C11347 Quantaurus - QY Absolute Photoluminescence Quantum Yield Spectrometer (Hamamatsu Photonics K.K), equipped with a 150 W Xenon lamp, an integrating sphere and a multi-channel detector.

Steady state emission and excitation spectra and photoluminescence lifetimes were obtained with a FLS 980 spectrofluorimeter (Edinburg Instrument Ltd.). Continuous excitation for the steady state measurements was provided by a 450 W Xenon arc lamp. Photoluminescence lifetime measurements were performed using an Edinburgh Picosecond Pulsed Diode Laser EPL-445 (Edinburg Instrument Ltd.), with central wavelength 442.2 nm and repetition rates 20 MHz, by time-correlated single-photon counting method.

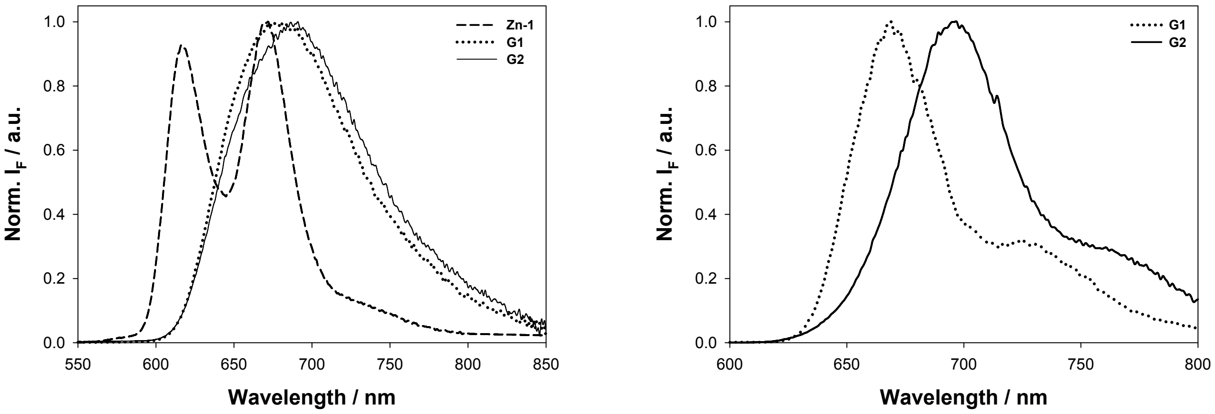

Figure S1. a) Fluorescence emission spectra of Zn-1, G1 and G2 in THF solution at RT (left); b) Fluorescence emission spectra of G1 and G2 in Toluene solution at 77K (right).

A remarkable bathochromic shift in the fluorescence emission spectra in THF solutions is highlighted for the new dyes G1 and G2 when compared with Zn-1. Two separated emission peaks at 617nm and 666nm are displayed for Zn-1 whilst a single broader emission band is observed at 679nm and 688nm for G1 and G2 respectively. These unstructured bands are probably ascribed to the rotational motions of bulky amino substituents in meso position, thus fluorescence spectra of G1 and G2 were also recorded at 77 K in Toluene (see Table S1). As a consequence, an intense peak at 669nm and a less intense one at 728nm are revealed for G1 and a further red-shifting of the emission bands is observed in case of G2 showing a maximum at 696nm with a shoulder at 762nm.

4) Theoretical DFT and TDDFT calculations

DFT and TDDFT calculations were performed on all of the investigated ZnII porphyrinates using Gaussian 09.[1] All of the structures were freely optimized *in vacuo* using the 6-311G(d) basis set, which was adopted on the basis of previous theoretical investigation on similar porphyrin derivatives.[2] The M06 functional[3] was chosen owing to its shown better performance in reproducing X-ray M-N (M=metal) bond lengths of metal-porphyrinates[4] with respect to the widely used B3LYP functional.[5-7] Single point calculations, including the solvent effects (THF and DMF) by means of the CPCM[8] conductor-like solvation model, were then performed on the optimized structures at the B3LYP/6-311G(d) level of theory in order to compute the energies and electronic distributions of the frontier orbitals. TD-B3LYP/6-311G(d) calculations were performed in THF on the optimized structures to determine the first singlet-singlet excitations. Up to 30 excitations were included in the TDDFT calculations. Results on the Zn-I complex show some little differences with respect to those previously reported[2] owing to both the slightly different computational protocol and the fact that the terbuthyl groups on the phenyl rings, previously replaced by H atoms, have here been considered.

Table S1. Experimental and computed electronic absorption spectra in THF solution of the Zn-porphyrins investigated in this work.

Dye	B bands λ_{abs} (nm) [log ε]	Computed B bands λ_{abs} (nm) [f]^a	Q1 band λ_{abs} (nm) [log ε]	Computed Q1 band λ_{abs} (nm) [f]^a	Q2 band λ_{abs} (nm) [log ε]	Computed Q2 band λ_{abs} (nm) [f]^a	Emission bands in THF (nm) [77K in Toluene]
Zn-1	438 [5.30]	431 [1.88] (56% H-1→L+2) (24% H→L+1) 424 [0.85] (36% H-1→L+1) (26% H-2→L)	568 [4.37]	521 [0.70] (42% H→L+2) (24% H-1→L)	608 [4.21]	628 [0.20] (94% H→L) 581 [0.32] (73% H-1→L)	617 666
	460(sh)	457 [1.09] (66% H-2→L)					
G1	457 [5.49]	441 [1.97] (38% H-6→L) (32% H-5→L+1) (27% H-4→L+2) 426 [1.99] (61% H-5→L+2) (32% H-4→L+1) 413 [0.49] (56% H-6→L)	575 [4.56]	554 [0.10] (64% H-4→L) 543 [0.27] (38% H-5→L) (37% H-1→L+2) 540 [0.41] (54% H-1→L+2) (32% H-5→L)	621 [4.53]	670 [0.10] (60% H→L) (33% H-1→L) 590 [0.23] (56% H→L+1) (22% H→L+2)	679 (broad) [669] [728](sh.)
G2	454 [5.33]	435 [1.25] (32% H-4→L+3) (27% H-5→L+2) 429 [1.76] (58% H-5→L+3) 402 [0.24] (54% H-6→L+2) (27% H-7→L) 395 [0.17] (88% H-6 →L+3)	574 [4.44]	505 [0.10] (37% H-3→L+2) 504 [0.31] (22% H-5→L+1) 498 [0.56] (70% H-6→L)	620 [4.39]	727 [0.07] (67% H→L) (22% H-1→L) 602 [0.41] (35% H→L+1) (27% H-5→L) 574 [0.59] (64% H→L+2) (28% H-5→L)	688(broad) [696] [762](sh.)

^{a} The oscillator strength f and the more important contributions (> 20%) to the transitions are reported in square and round brackets, respectively. Only transitions with $f \geq 0.07$ are reported.

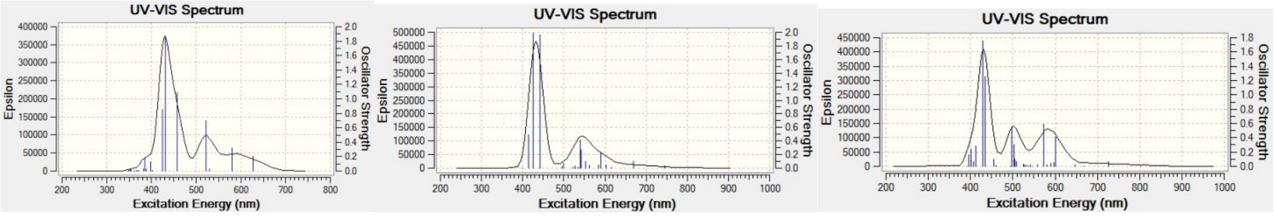

Figure S2. CPCM- TD-B3LYP/6-311G(d) absorption spectra of compounds Zn-1 (left), G1 (center) and G2 (right) in THF, resulting from convolution of the excitation energies with 0.10 eV of half-bandwidth.

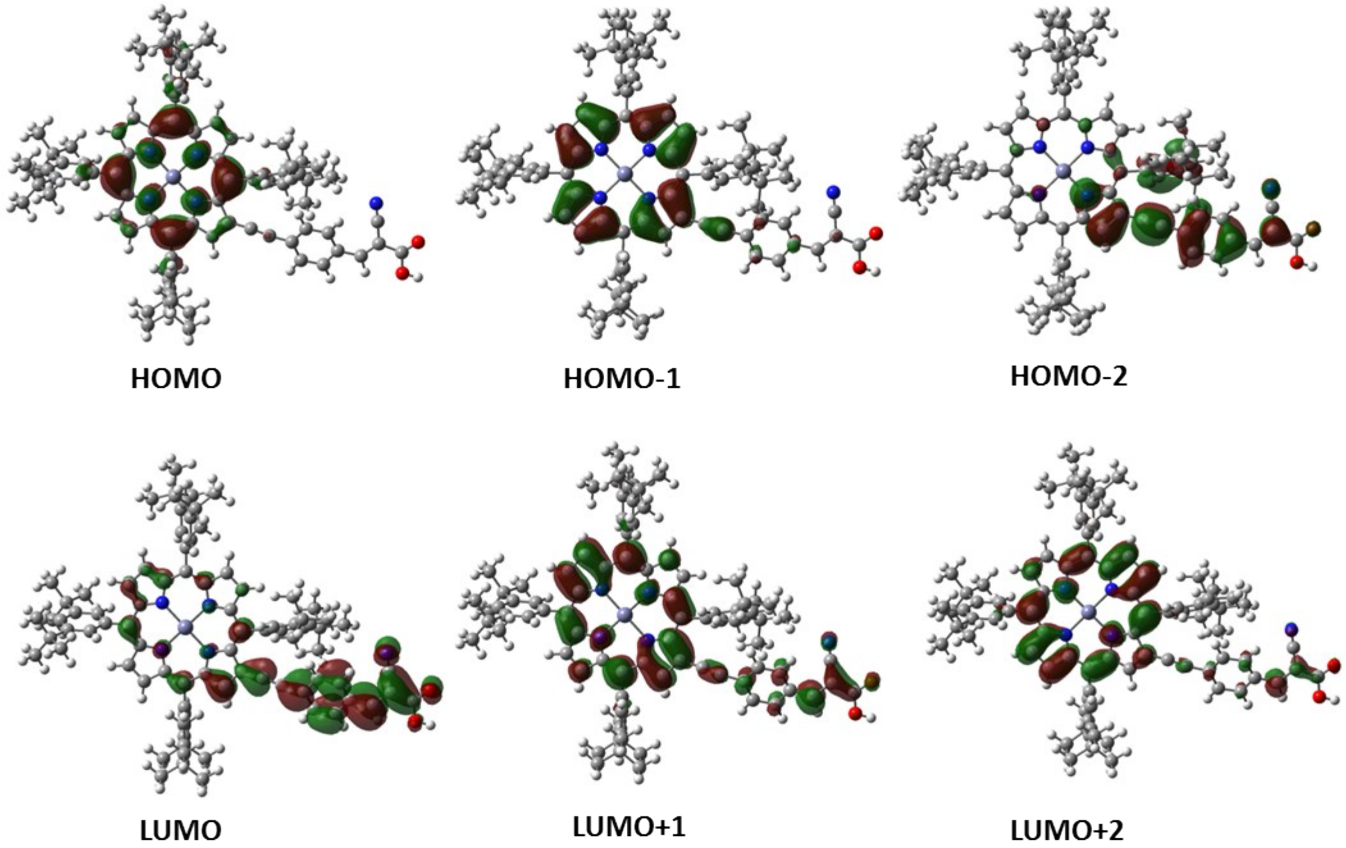

Figure S3. Isodensity plots of the B3LYP/6-311G(d) MOs computed in THF mainly involved in the lowest energy transitions of Zn-1 (Isosurfaces value 0.02).

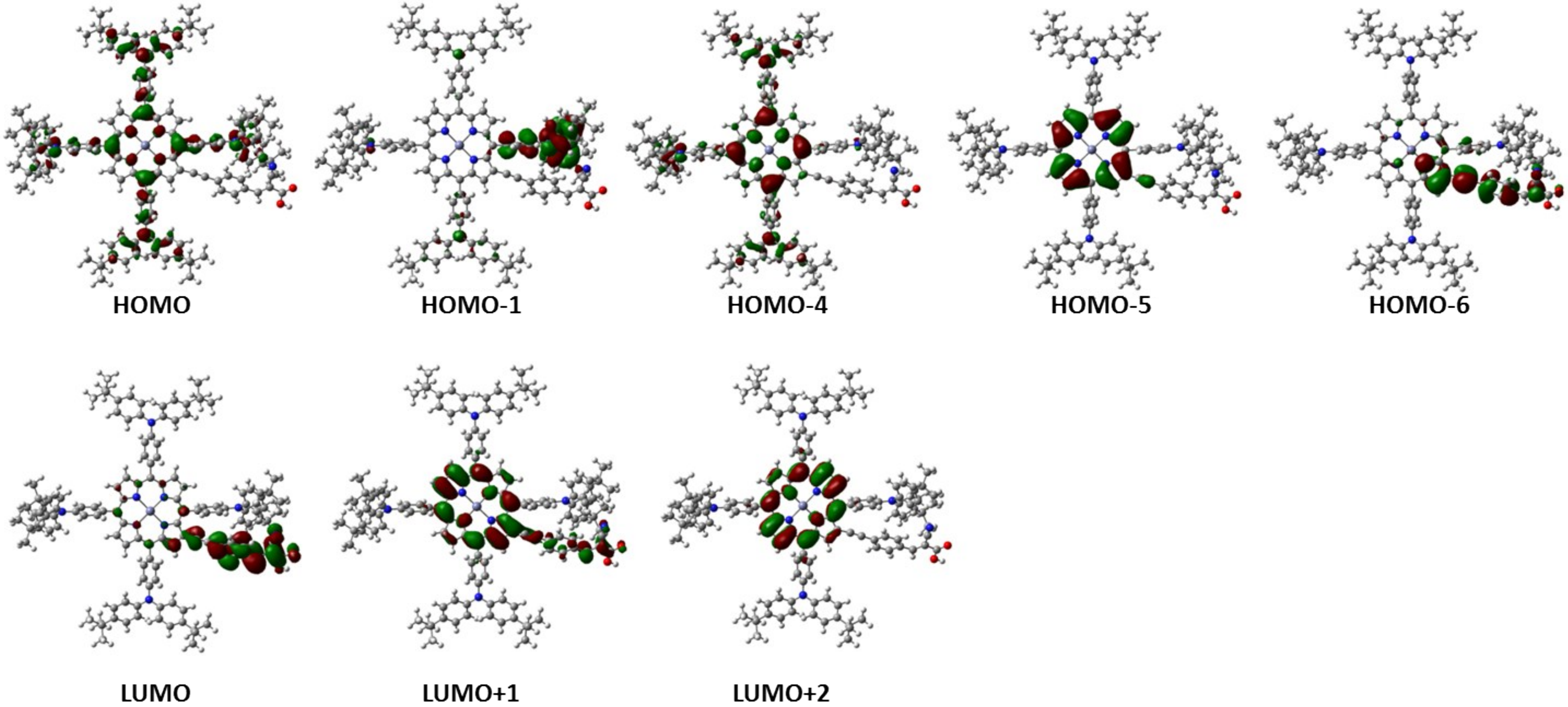
HOMO HOMO-1 HOMO-4 HOMO-5 HOMO-6

LUMO LUMO+1 LUMO+2

Figure S4. Isodensity plots of the B3LYP/6-311G(d) MOs computed in THF mainly involved in the lowest energy transitions of G1 (Isosurfaces value 0.02).

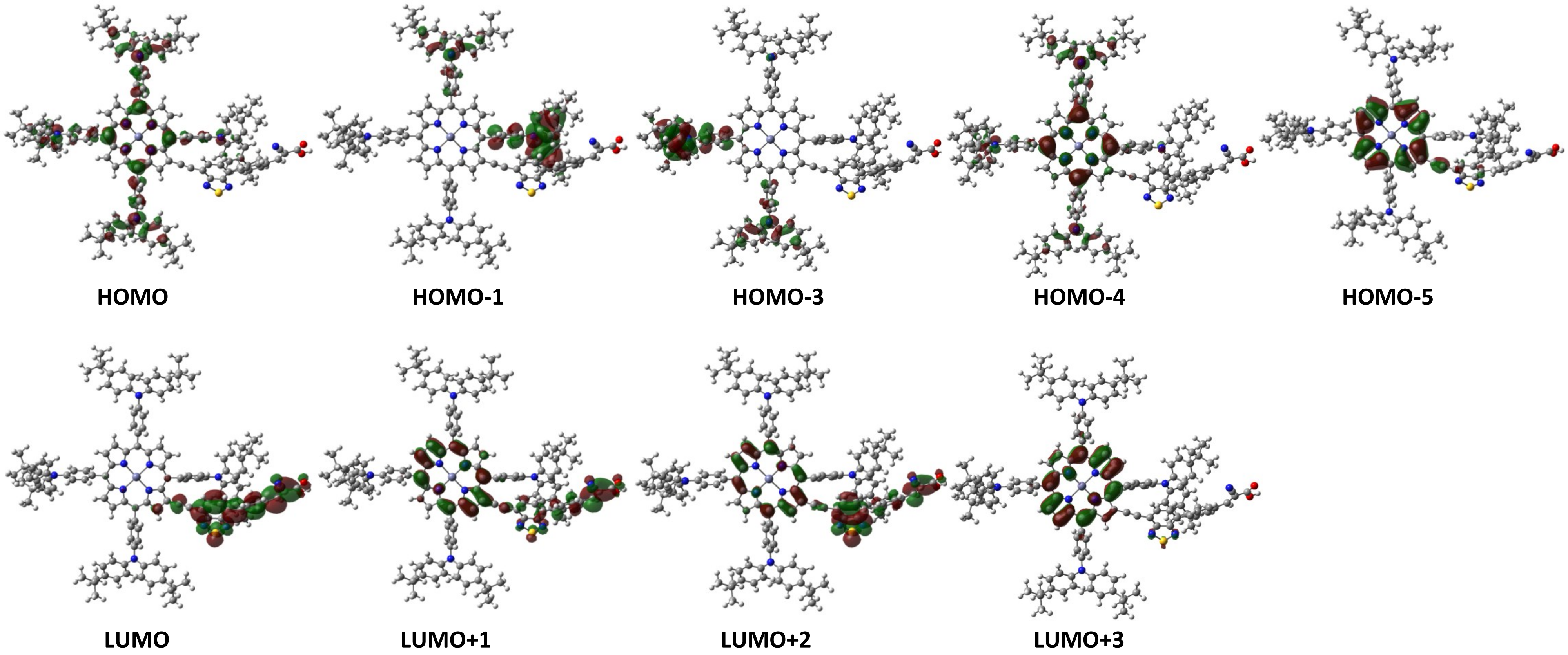

Figure S5. Isodensity plots of the B3LYP/6-311G(d) MOs computed in THF mainly involved in the lowest energy transitions of G2 (Isosurfaces value 0.02).

5) Electrochemical measurements

The voltammetric studies have been performed in a 4 cm^3 cell, in 5×10^{-4} - 10^{-3} M solutions in dimethylformamide (Aldrich, 99.8%) with 0.1 M tetrabutylammonium perchlorate (TBAP, Fluka) as the supporting electrolyte. The solutions were de-aerated by N_2 bubbling. The ohmic drop has been compensated by the positive feedback technique.[9]

Cyclic voltammetry (CV) and Differential Pulse Voltammetry (DPV) experiments were carried out using an AUTOLAB PGSTAT potentiostat (EcoChemie, The Netherlands) run by a PC with GPES software. CV investigation was carried out at scan rates typically ranging 0.05 to 2 Vs^{-1}, with ohmic drop compensation. The working electrode was a glassy carbon one (AMEL, diameter = 1.5 mm) cleaned by synthetic diamond powder (Aldrich, diameter = 1 μm) on a wet cloth (STRUERS DP-NAP); the counter electrode was a platinum disk or wire. The operating reference electrode was an aqueous saturated calomel electrode, but the potentials were ultimately referred to the Fc^+/Fc (ferrocinium/ferrocene) couple (the intersolvental redox potential reference currently recommended by IUPAC[10, 11] by both external and internal standardization). To prevent water and chloride leakage into the working solution a compartment filled with the operating medium and ending with a porous frit was interposed between the reference electrode and the cell. CV curves of G1 and G2 are reported in figures S6 and S7, while DPV analysis of the same dyes is reported in fig. S8. The anodic and cathodic processes are investigated separately to avoid any contamination or corruption by possible opposite electron-transfer processes. Starting from the whole anodic (or cathodic) scan we reduce the potential window step-by-step in order to investigate every single electronic process. The red/blue curves were adopted to highlight the first oxidation/reduction process. In both cases the first oxidation and reduction peaks are reversible or quasi-reversible from both the electrochemical and chemical point of view, affording the determination of formal potentials ($E°'$ approximate standard potential $E°$ under the assumption of neglecting activity coefficients). The electrochemical HOMO and LUMO energy levels, and thus the HOMO-LUMO energy gap (*Eg*) were evaluated from the $E°'$ values (Table S2 and Table 1).[12]

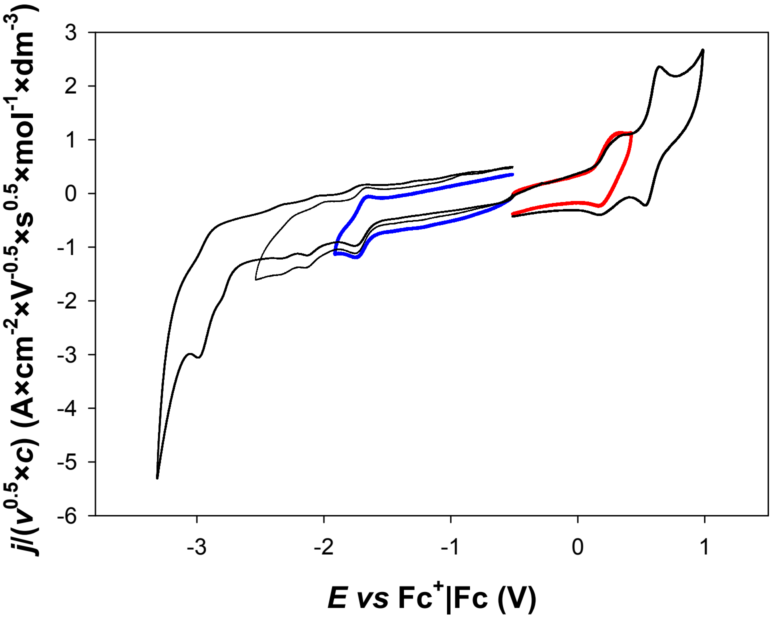

Figure S6. CV pattern of **G1** on glassy carbon electrode, in DMF + 0.1 M TBAP, at 0.2 Vs^{-1}; first anodic process is highlighted in red and first cathodic process in blue.

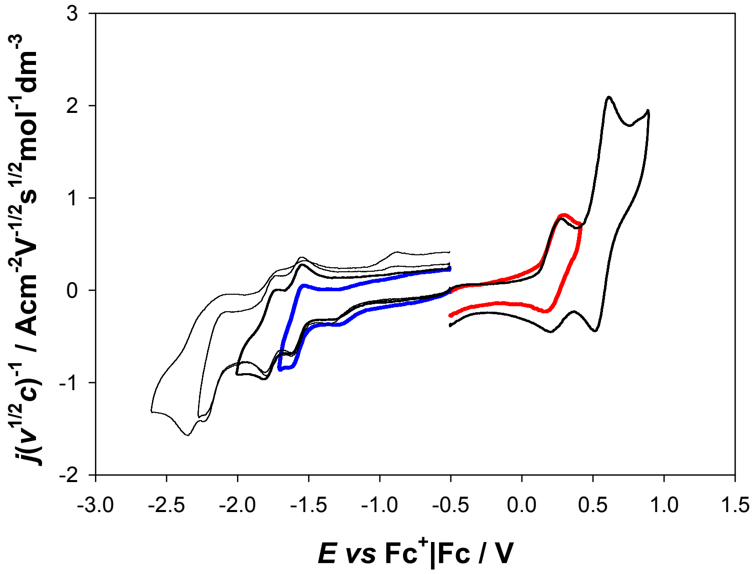

Figure S7. CV pattern of **G2** on glassy carbon electrode, in DMF + 0.1 M TBAP, at 0.2 Vs^{-1}; first anodic process is highlighted in red and first cathodic process in blue.

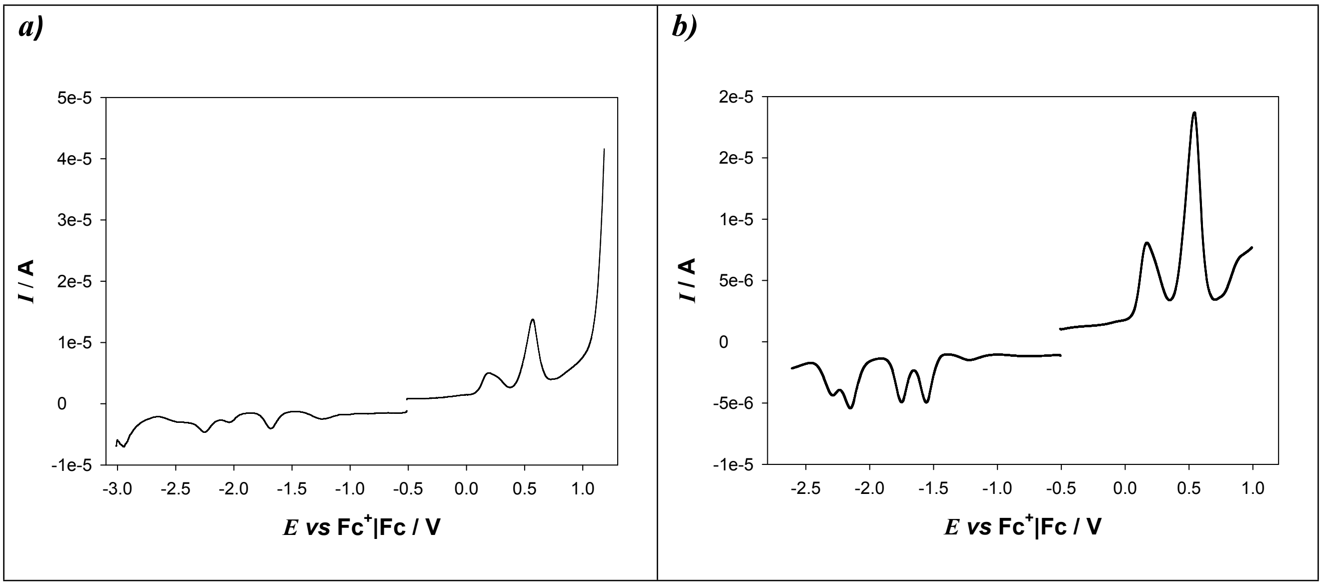

Figure S8. DPV pattern of **G1** (*a*) and **G2** (*b*) on glassy carbon electrode, in DMF + 0.1 M TBAP.

Table S2. Key CV features and the electrochemical energy levels HOMO and LUMO derived therefrom. $E°_{Ic}$ and $E°_{Ia}$ (or $E_{p,Ic}$ and $E_{p,Ia}$) all referred to the ferrocene couple.[10, 11]

	$E_{p,Ia}$/V (Fc$^+$|Fc)	$E°'_{Ia}$/V (Fc$^+$|Fc)	$E_{p,Ic}$/V (Fc$^+$|Fc)	$E°'_{Ic}$/V (Fc$^+$|Fc)	HOMO/eV	LUMO/eV	$E°'$/V ($E_{g,EC}$/eV)
Zn-1[2]	0.35	0.32	-1.72	-1.69	-5.12	-3.11	2.02
G1	0.31	0.24	-1.74	-1.70	-5.04	-3.10	1.94
G2	0.29	0.23	-1.65	-1.60	-5.03	-3.21	1.82

6) DSSCs fabrication and evaluation

TiO_2 electrodes were prepared by spreading (doctor blading) a colloidal TiO_2 paste (20 nm sized; "Dyesol" DSL 18NR-T) onto a conducting glass slide (FTO, Hartford glass company, TEC 8, having a thickness of 2.3 mm and a sheet resistance in the range 6–9 Ω/cm^2) that had been cleaned with water and EtOH treated with a plasma cleaner at 100 W for 10 min, dipped in a freshly prepared aqueous $TiCl_4$ solution (4.5×10^{-2} M), at 70 °C, for 30 min, and finally washed with ethanol. After a first drying at 125 °C for 15 min, a reflecting scattering layer containing >100 nm sized TiO_2 ("Solaronix" Ti-Nanoxide R/SP) was bladed over the first TiO_2 coat and sintered until 500 °C for 30 min. Then, the glass coated TiO_2 was dipped again into a freshly prepared aqueous $TiCl_4$ solution (4.5×10^{-2} M), at 70 °C for 30 min, then washed with ethanol, and heated once more at 500 °C for 15 min. At the end of these operations, the final thickness of the TiO_2 electrode was in the range 8-12 μm, as determined by SEM analysis. After the second sintering, the FTO glass coated TiO_2 was cooled at about 80 °C and immediately dipped into a CH_2Cl_2 solution [2.0×10^{-4} M] of the selected dye at r.t. for 20 h. The dyed titania glasses were washed with EtOH and dried at r.t. under a N_2 flux. Finally, the excess of TiO_2 was removed with a sharp Teflon penknife, and the exact active area of the dyed TiO_2 was calculated by means of microphotography. A 50 μm thick Surlyn spacer (TPS 065093-50 from Dyesol) was used to seal the photoanode and a platinized FTO counter electrode. Then, the cell was filled up with the desired electrolyte solution. The photovoltaic performance of the cells was measured with a solar simulator (Abet 2000) equipped with a 300 W xenon light source; the light intensity was adjusted with a standard calibrated Si solar cell ("VLSI Standard" SRC-1000-RTD-KG5). The current-voltage characteristics were acquired by applying an external voltage to the cell and measuring the generated photocurrent with a "Keithley 2602A" (3A DC, 10A Pulse) digital source meter. The complete results are summarized in Table S3. The IPCE measurements were performed with a Bentham PVE300 instrument equipped with a QTH xenon lamp and a Stanford SR830 DSP lock-in amplifier, in DC mode without chopper and bias, in the dark with monochromatic light from 300 to 900 nm.

The integration of the IPCE response with respect to the solar irradiation spectrum results in Jsc values corresponding to 83 - 91% of the values measured under sAM 1.5 simulated solar illumination and in the presence of a black mask. Such differences are not quite unusual for DSSCs and similar results were observed with organic metal-free sensitizers too.[13]

Table S3. Main photovoltaic characteristics of the DSSC based on the porphyrinic dyes Zn-1, G1 and G2, under standard AM 1.5 simulated solar illumination and in the presence of a black mask of *ca.* 12 mm^2 aperture. Dyes dissolved in CH_2Cl_2 [0.2 mM]. Electrolyte composition: 0.6 M N-methyl-N-butylimidazolium iodide, 0.04 M iodine, 0.025 M LiI, 0.05 M guanidinium thiocyanate, 0.28 M tert-butylpyridine in 15/85 (v/v) mixture of valeronitrile/acetonitrile.

DYE	Device number	Loading time (h)	η	FF	Voc (V)	Jsc (mA/cm2)
Zn-1	1	20	**5.36**	68.8	0.683	11.41
	2	20	**4.66**	71.9	0.656	9.88
	3	20	**5.62**	70.6	0.690	11.53
	4	20	**4.91**	69.1	0.685	10.36
	5	20	**4.97**	69.9	0.686	10.37
Zn-1+CDCA[a]	6	1	**3.49**	74.1	0.627	7.52
	7	2	**3.78**	72.9	0.607	8.54
	8	20	**4.64**	73.9	0.643	9.77
G1	9	20	**2.46**	65.0	0.584	6.47
	10	20	**2.30**	68.2	0.561	6.02
	11	20	**2.72**	69.4	0.580	6.77
	12	20	**2.40**	65.1	0.581	6.35
G1+CDCA[a]	13	1	**2.36**	72.2	0.603	5.43
	14	2	**1.99**	71.5	0.589	4.73
	15	20	**1.19**	68.2	0.558	3.13
G2	16	20	**4.14**	68.6	0.650	9.29
	17	20	**4.25**	67.5	0.638	9.88
	18	20	**4.37**	68.0	0.656	9.87
	19	20	**4.08**	65.6	0.637	9.77
	20	20	**4.18**	67.2	0.655	9.49
G2+CDCA[a]	21	20	**6.18**	72.2	0.668	12.81
	22	20	**6.22**	72.6	0.681	12.58
	23	20	**6.21**	72.0	0.668	12.95
	24	20	**6.13**	73.0	0.682	12.31
Zn-1[b]	25	1	**2.98**	73.8	0.613	6.59
	26	2	**3.76**	73.2	0.611	8.41
	27	20	**3.85**	72.5	0.634	8.39
G1[b]	28	1	**3.07**	72.9	0.610	6.91
	29	2	**3.41**	72.4	0.613	7.69
	30	20	**3.84**	71.8	0.606	8.83
G2[b]	25	20	**4.16**	69.8	0.602	9.90
	26	20	**4.32**	70.4	0.618	9.93
	27	20	**3.88**	67.6	0.597	9.63
	28	20	**4.00**	67.8	0.618	9.56

---

[a] Dye : CDCA = 1 : 10, mol

[b] Dyes dissolved in a mixture toluene : EtOH (1:1, *v/v*) [0,2 mM]

7) Electrochemical impedance spectroscopy (EIS)

EIS measurements were performed at different bias potentials by using a AUTOLAB PGSTAT 302N potentiostat with FRA module (EcoChemie, The Netherlands) in a frequency range between 10^5 Hz and 0.1 Hz, under 1 sun illumination by using a PET SS50AAA-TP solar simulator with an AM1.5 G filter calibrated to 100 mW × cm^2 using as a reference a Silicon standard solar cell. The resulting EIS spectra were fitted with the ZView software (Scribner Associates) and analysed through the equivalent circuit here below reported.[14]

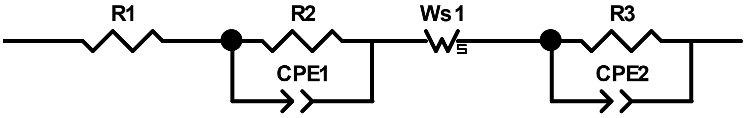

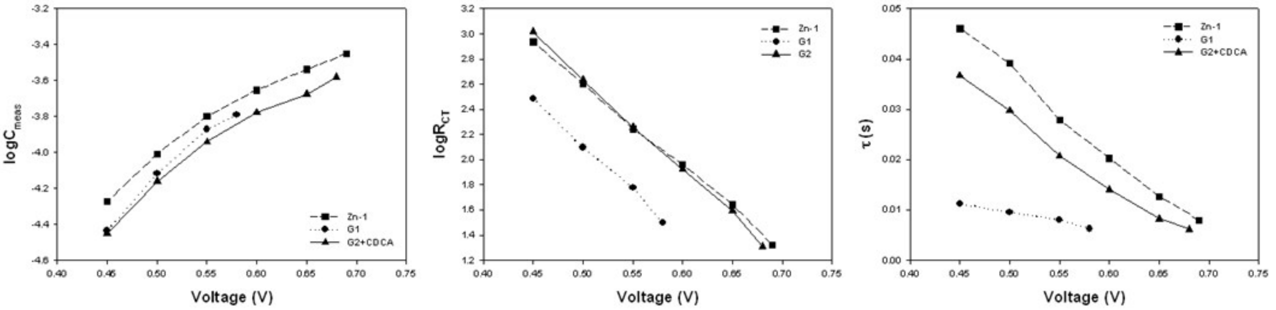

Figure S9. Chemical Capacitance (a), Charge Transport Resistance (b) and Apparent Electron Lifetime as a Function of the Corrected Potential for the Investigated Dyes under Illumination.

8) Dye-loading measurements

Dye-loading measurements were carried out recording the UV-vis spectra of dye-sensitized 5-µm transparent TiO_2 films with a Shimadzu UV3600 spectrophotometer and using as a reference a 5-µm transparent TiO_2 film not sensitized. A black-paper mask was applied to analyze only the beam passing through the film. The transparent films of TiO_2 were prepared by screen-printing (Aurel Automation C900 Screen-Stencil Printer) of a commercial transparent TiO_2 paste (Dyesol 18NR-T) onto the conductive side of a FTO glass of 2.2 mm thick.

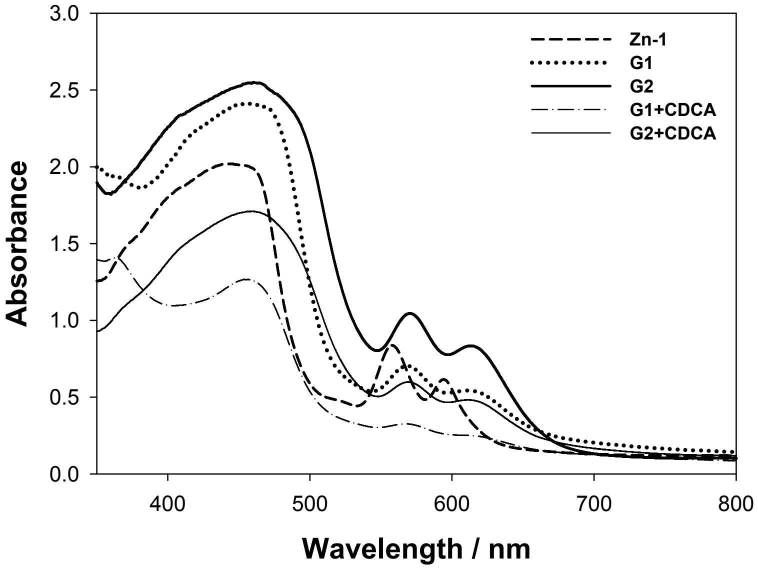

Figure S10. UV-vis spectra of 5-µm transparent TiO_2 films sensitized with the dyes investigated.

The surface concentration (Γ of the three dyes Zn-1, G1 and G2, were calculated according to the following equation:

$$A = 1000 \cdot \varepsilon \cdot \Gamma$$

Table S4. Dye loading of Zn-1, G1 and G2 on transparent TiO2 films.

	ε[a] (m^2/mol)	***A*** (a.u)	**Γ** (mol/cm^2)
Zn-1	23500	0.837	$3.56 \cdot 10^{-8}$
G1	36220	0.703	$1.94 \cdot 10^{-8}$
G2	27777	1.046	$3.76 \cdot 10^{-8}$

[a] It is referred to Q1 band: 568nm (Zn-1); 575nm (G1); 574nm (G2).

References

1. M. J. Frisch, G. W. Trucks, H. B. Schlegel, G. E. Scuseria, M. A. Robb, J. R. Cheeseman, G. Scalmani, V. Barone, B. Mennucci, G. A. Petersson, H. Nakatsuji, M. Caricato, X. Li, H. P. Hratchian, A. F. Izmaylov, J. Bloino, G. Zheng, J. L. Sonnenberg, M. Hada, M. Ehara, K. Toyota, R. Fukuda, J. Hasegawa, M. Ishida, T. Nakajima, Y. Honda, O. Kitao, H. Nakai, T. Vreven, J. A. Montgomery, J. E. Peralta, F. Ogliaro, M. Bearpark, J. J. Heyd, E. Brothers, K. N. Kudin, V. N. Staroverov, R. Kobayashi, J. Normand, K. Raghavachari, A. Rendell, J. C. Burant, S. S. Iyengar, J. Tomasi, M. Cossi, N. Rega, J. M. Millam, M. Klene, J. E. Knox, J. B. Cross, V. Bakken, C. Adamo, J. Jaramillo, R. Gomperts, R. E. Stratmann, O. Yazyev, A. J. Austin, R. Cammi, C. Pomelli, J. W. Ochterski, R. L. Martin, K. Morokuma, V. G. Zakrzewski, G. A. Voth, P. Salvador, J. J. Dannenberg, S. Dapprich, A. D. Daniels, O. Farkas, J. B. Foresman, J. V. Ortiz, J. Cioslowski and D. J. Fox, *Gaussian 09, Revision D.01,Gaussian Inc.,* Wallingford CT, **2013**.
2. G. Di Carlo, A. Orbelli Biroli, M. Pizzotti, F. Tessore, V. Trifiletti, R. Ruffo, A. Abbotto, A. Amat, F. De Angelis and P. R. Mussini, *Chem. - Eur. J.*, 2013, **19**, 10723-10740.
3. Y. Zhao and D. G. Truhlar, *Theor. Chem. Acc.*, 2008, **120**, 215-241.
4. G. Di Carlo, A. Orbelli Biroli, F. Tessore, S. Rizzato, A. Forni, G. Magnano and M. Pizzotti, *J. Org. Chem.*, 2015, **80**, 4973-4980.
5. A. D. Becke, *The Journal of Chemical Physics*, 1993, **98**, 5648-5652.
6. C. Lee, W. Yang and R. G. Parr, *Physical Review B*, 1988, **37**, 785-789.
7. B. Miehlich, A. Savin, H. Stoll and H. Preuss, *Chem. Phys. Lett.*, 1989, **157**, 200-206.
8. M. Cossi, N. Rega, G. Scalmani and V. Barone, *J. Comput. Chem.*, 2003, **24**, 669-681.
9. A. J. Bard and L. R. Faulkner, eds., *Electrochemical Methods. Fundamentals and Applications.*, Wiley, New York, 2002.
10. G. Gritzner and J. Kuta, *Pure Appl. Chem.*, 1984, **56**, 461-466.
11. G. Gritzner, *Pure Appl. Chem.*, 1990, **62**, 1839-1858.
12. P. R. Mussini, A. Orbelli Biroli, F. Tessore, M. Pizzotti, C. Biaggi, G. Di Carlo, M. G. Lobello and F. De Angelis, *Electrochim. Acta*, 2012, **85**, 509-523.
13. D. Demeter, J. Roncali, S. Jungsuttiwong, F. Melchiorre, P. Biagini and R. Po, *J. Mater. Chem. C*, 2015, **3**, 7756-7761.
14. S. Carli, E. Busatto, S. Caramori, R. Boaretto, R. Argazzi, C. J. Timpson and C. A. Bignozzi, *J. Phys. Chem. C*, 2013, **117**, 5142-5153.